Influence of ZnO on Electrochemical and Physiochemical Properties of Lanthanum Strontium Cobalt Ferrite as Cathode for Intermediate Temperature Solid Oxide Fuel Cells

Ahmad Fuzamy Mohd Abdul Fatah[1], Ahmad Azmin Mohamad[2], Muhammed Ali S.A.[3], Andanastuti Muchtar[3], Nor Anisa Arifin[3], Wan Nor Anasuhah Wan Yusoff[3], Noorashrina A. Hamid[1*]

[1]School of Chemical Engineering, Engineering Campus, Universiti Sains Malaysia, 14300 Nibong Tebal Penang, Malaysia
[2]School of Materials & Mineral Resources, Engineering Campus, Universiti Sains Malaysia, 14300 Nibong Tebal Penang, Malaysia
[3]Fuel Cell Institute, Universiti Kebangsaan Malaysia, UKM, 43600 Bangi, Selangor, Malaysia

Abstract. This study investigates the impact of zinc oxide on the physical characteristics and electrochemical behavior of the LaSrCoFe (LSCF) cathode. Electrochemical impedance spectra in conjunction with the bode phase were used to optimize the amount of zinc oxide addition in the LSCF cathode. Brunauer-Emmett-Teller (BET) and thermal analysis were utilized to substantiate the electrochemical discovery that the LSCF: ZnO ratio yields rational oxygen reduction reaction and stoichiometric outcomes. Initial characterization, comprising of phase and bonding analyses, indicated that LSCF-ZnO was successfully synthesized at 800 ℃ using an improved modified sol-gel technique. The addition of 5% zinc oxide to LSCF results in the lowest overall area-specific resistance (ASR) rating. The Bode phase implies that the addition of 5% zinc oxide to LSCF reduces the low-frequency impedance by 64.28%, indicating that the cathode experienced a greater oxygen reduction reaction. After the addition of 5% zinc oxide, a single LSCF-ZnO cell may function at temperatures as low as 650 °C, and the LSCF cathode power density is increased by 25.35%. The surface morphology of the LSCF-ZnO cathode reveals an overall particle size of less than 100 nm, and mapping analysis reveals a homogeneous distribution of ZnO over the cathode layer. Consequently, LSCF-ZnO demonstrated outstanding chemical compatibility between LSCF and ZnO, bonding characteristics, and electrochemical performance with the capacity to function at an intermediate temperature (600 °C – 800 °C).

Keywords: Active surface area; Intermediate temperature solid oxide fuel cell; LSCF-Zinc oxide; Oxygen reduction reaction

1. Introduction

Fuel is a substance that is utilized to produce energy. Since the beginning of the 20th century, mankind has relied on fuel for their daily needs. Due to their high energy output and convenience, non-renewable energy sources have gained tremendous attention as it's in line with the world agenda of reducing carbon footprint by 2030. People are growing

increasingly interested in renewable energy as they become more aware of the depletion of fossil resources and recent environmental disputes. Intermediate temperature solid oxide fuel cell (IT-SOFCs) is an efficient, ultra-clean green technology device capable of converting chemical energy into electrical energy by adapting the oxygen reduction reaction (ORR) technique at intermediate temperature (600 °C – 800 °C). IT-SOFCs are also capable of producing a stable reaction in term of long-term stability, low carbon emission, and fuel flexibility (Abd-Aziz et al., 2020).

In IT-SOFCs, the cathode electrode plays an important role in oxygen reduction reaction particularly. Chemical compatibility among cathode compositions is the most important property of MIEC-type materials used in IT-SOFCs (Wu and Ghoniem, 2019). Nowadays, lanthanum, strontium, cobalt, and ferrite (LSCF) have been used in IT-SOFCs (Tahir et al., 2022). The oxygen ions mainly transport ions in the lattice oxide at the interface of the cathode and electrolyte (Jiang, 2019). Infiltrations of novel transition metals can create oxygen vacancies, namely ZnO. In the ABO_x perovskite, the bulk oxygen vacancies formation is reported to be facilitated with a small amount of metal content (Guo et al., 2015).

It has been observed that zinc oxide has good stability at intermediate temperatures operation, can act as a sintering aid, and has a potential catalytic activity that increases the oxygen reduction reaction rate and active surface area at the cathode (Rafique et al., 2019; Abbas et al., 2019; Adiwibowo et al., 2018). Although the addition of zinc oxide causes extrinsic defects or impurities, the disadvantage has been mitigated by establishing a good ratio of zinc oxide in the composition (Omari, Omari, and Barkat, 2018). It has also been found that zinc oxide is chemically compatible with ceria-based electrolytes, and it could have influenced the ORR process at intermediate temperatures (Xu et al., 2020). In addition, the inclusion of zinc oxide minimizes the likelihood of the cathode interacting with carbon dioxide during the oxygen reduction reaction (Rafique et al., 2019).

In addition, zinc oxide is typically promising in terms of performance and stability in SOFCs (Kusdianto et al., 2019; Hajmohammadi et al., 2017). It has been reported that the addition of zinc improves the triple boundary phase on the cathode side, allowing it to operate within the working range of IT-SOFCs (Abbas et al., 2019). Solid oxide fuel cells (SOFCs) favor a big triple boundary phase and high ORR process, especially on the cathode side, because high ionic conduction in electrolytes and electrodes is directly proportional to promising power output (Xu et al., 2022). It has been observed that the use of zinc oxide as a cathode produces a promising power density of approximately 500 mW^{-1} cm^{-2} at an operating temperature of 550 °C, which falls within the range of intermediate temperatures (Shah et al., 2019). Moreover, zinc oxide also reduced polarisation losses by enhancing the ORR rates on the cathode (Hussain et al., 2019). However, there is no analysis yet regarding the addition of ZnO toward LSCF as well as the electrochemical evaluation of LSCF-ZnO composite cathode. Therefore, this study is focusing on fabricating the LSCF-ZnO cathode via modified sol-gel route, whereas the EIS analysis was conducted with an intermediate temperature range (600 °C – 800 °C).

2.   Methods

All chemicals used were purchased from Sigma Aldrich®, Malaysia, and applied without additional purification. The precursor of LSCF was formed via the sol-gel method under controlled conditions. The nitrate metal salt consisting of LSCF (ratio 6:4:2:8) was mixed in a 50 mL beaker, and excess ethylene glycol was added to dissolve the metal salt. The chelating agent was mixed into the solution with the following ratio: metal salt: citric acid: EDTA (1:1:2). The initial pH solution was measured at the beginning while the metal

salt solution was stirred continuously at 100 rpm. After dissolving the metal salt and chelating agent in ethylene glycol, the ammonium solution was added using a titration technique until the pH of the solution reached approximately 7. The mixture was heated for 8 hours at 100 °C to promote gel formation. The gel was calcined at 800 °C for 6 hours. The resultant fine powder LSCF and zinc oxide were mixed with a ratio of 1:1 in excess acetone and sintered at 800 °C for compatibility characterization. The same batch of LSCF containing 3wt.%, 5wt.%, and 7wt.% of zinc oxide was prepared to measure the specific surface area.

The fine GDC powder was produced via a conventional sol-gel process and sieved for powder uniformity. The GDC pellet was produced using the pellet-pressing method with a 25 mm diameter stainless-steel mold at 300 MPa, followed by sintering at 1400 °C for 6 hours. The cathode ink was designed with a combination of LSCF-ZnO and vehicle ink at a ratio of 1:1.5. The vehicle ink was formed with a mixture of ethyl cellulose and terpineol at a ratio of 5% ethyl cellulose to 95% terpineol. Cathode ink was applied on both sides of the electrolyte surface (1 cm diameter) using screen printing and sintered at 1100 °C for 2 hours for symmetric cells. The electrochemical performance was assessed via an electrolyte-supported single cell with a NiO-GDC anode. A NiO-GDC (40:60 ratio) slurry was applied on one side of the GDC electrolyte surface, approximately 1 cm in diameter, using screen printing and sintered at 1300 °C for 2 hours. The cathode on a single cell was fabricated in the same manner as the symmetric cell.

2.1. Characterization Procedure

Bonding analysis of precursor LSCF till LSCF-ZnO powder was zanalyzed via FTIR Spectrometer (Shimadzu model IR Prestige-21) from 400 cm^{-1} to 1700 cm^{-1}. The phase composition of LSCF, LSCF-ZnO, and ZnO was characterized using X-ray diffraction (XRD) AXS Bruker GmbH from 10° to 90° with Cu Kα radiation. The specific surface area of the LSCF-ZnO was evaluated using Brunauer–Emmett–Teller (BET) with an average amount of 0.5 grams per sample. The Scanning Electron Microscopy (SEM) analysis was conducted toward LSCF-ZnO symmetrical cells using Regulus 8220®. The acceleration voltage was 5kV using backscattering electron and scattering electron (BSE+SE), and the magnification used was 30k. The particle size was measured using the software available in Regulus 8220® for 70 readings.

The thermal decomposition behavior analysis of the LSCF-ZnO was conducted using a TGA zanalyzer model Pelkin Elmer STA 600®, from 30 °C to 800 °C with a heating rate of 5 °C/min in air and air flowrate of 50 cm^3/min. For calcined composited cathode powder, the value of oxygen stoichiometric was calculated via equation 1 (Samreen *et al.,* 2020). $\Delta m/m_s$ refers to weight loss of the material, M_{sample} represent the molecular weight of the sample, M_{oxygen} refers to molecular weight of oxygen.

$$\Delta\delta = \Delta m \frac{M_{Sample}}{m_s M_{Oxygen}} \tag{1}$$

The Electrochemical Impedance Spectra (EIS) analysis was used together with the furnace system (PGSTAT302N, Metrohm Autolab®). The electrode surface was coated with silver paste, and silver wires were attached to the electrodes for measuring the cathode resistance. The symmetric cell was evaluated using Digi-Sense digital thermocouple meter (Eutech Instruments) with type-K thermocouple. The temperature for the EIS varies from 600 °C to 800 °C, with signal amplitude of 10 mv and frequency range from 0.1 Hz to 1 MHz. NOVA®-software (Version 1.10) was utilized to zanalyze the response data to the equivalent circuit, and each output data were plotted using Origin software. The analysis was conducted in the open air for symmetric cells. The single cell was evaluated using a fuel mixture of 10 % hydrogen and 90 % nitrogen at the anode side, with a flow rate of 25

mL/min. The cathode side was supplied with air at the same flow rate. The impedance spectra for single cells were recorded with 10 mV AC signal perturbation under open-circuit conditions. The stabilizing time was 1 hour. Area-specific resistance (ASR) for the symmetric cell was calculated via equation 2, where the Rp refers to polarization resistance, and S refers to the working area of the cathode (Dumaisnil *et al.*, 2014).

$$ASR = \frac{R_p.S}{2}$$
(2)

3. Results and Discussion

3.1. LSCF-ZnO Powder Characterization

Figure 1 (a) shows the XRD diagram for LSCF, ZnO, and LSCF-ZnO composite fabricated at 800 °C. In the LSCF-ZnO composite powder, each peak was distinguished as LSCF and zinc oxide. The LSCF-ZnO powder consists of a mixture of two crystalline phases, namely LSCF (JCPDS: 48-0124) and ZnO (JCPDS: 79-2205), generating perovskite and hexagonal structure, respectively. The cell parameters of LSCF are a =b = 0.549 nm, c = 13.375 nm, and zinc oxide cell parameters are a = b = 0.325 nm, c = 0.521 nm. No tertiary phase was detected, indicating good compatibility between LSCF and zinc oxide, as well as high purity.

Figure 1 (b) explains the carbonate bond existence from LSCF calcined at 600 ^{0}C to LSCF-ZnO calcined at 800 °C to show the reduction of carbonate bond existence in A-site. The vibration mode of carbonate ion is described as the band between 600 and 1100 cm^{-1}, whereas the band between 1400 and 1700 cm^{-1} resembles the symmetrical and asymmetrical stretching modes of carbonate bond, which in this case is attributed to the formation of SrCo$_3$. No increase in intensity was detected for the A-site after the addition of zinc oxide, indicating that 800 °C is a suitable calcination temperature for LSCF-ZnO processing. This conclusion is supported by the absence of an additional carbonate peak following the addition of ZnO to LSCF. The small intensity, which is categorized as carbonate trace intensity, also showed that the sample had sufficient calcination temperature, which contributed to a high-purity sample where the carbon was almost removed from the sample. It is important to keep the carbonate level low because carbon can build up during ion exchange and block the pores. This lowers the electrochemical performance because the porous structure could provide a fast path for ions to move. Thus, calcination temperatures of 600 °C – 800 °C were chosen based on the analysis of XRD and FTIR that implies the existence of carbonate bond as well as high purity of LSCF-ZnO.
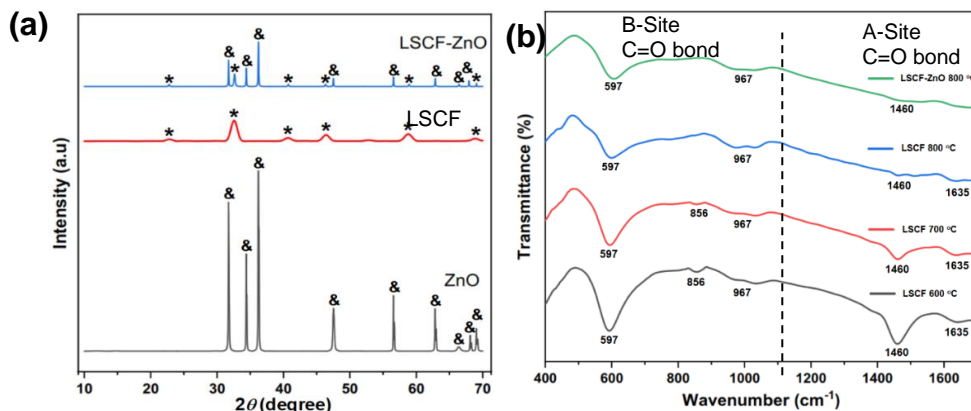

Figure 1 XRD pattern for the powder of LSCF, ZnO and LSCF-ZnO (a) FTIR spectra of LSCF powder calcined at 600 °C, 700 °C and 800 °C and LSCF with 5 wt.% of ZnO (b)

SEM micrographs of LSCF and LSCF with the addition of 5 wt% ZnO electrode surface are shown in Figure 2 (a and b). As depicted in the images, it was agreed that LSCF and LSCF-ZnO sintered at 1100 °C produced spheres that were well connected to each other and subsequently produced a porous network. It is also depicted similarly to other articles, stating a honeycomb-like structure, which is essential to the ORR process. The concept behind metal oxide addition is for the metal oxide to reduce the agglomeration effect, as seen in Fig. 3b. These findings were also published in several articles on the addition of metal oxide to the cathode (dos Santos-Gómez *et al.*, 2018; Nadeem *et al.*, 2018; Gao *et al.*, 2017). As the O^{2-} ions flow between the LSCF and ZnO without passing through an air gap, the metal oxide will cover the gap and promote the ORR process. It was discovered that the particle size distribution of LSCF-ZnO is much more uniform, ranging from 70 nm to 100 nm, compared to LSCF, which has a particle size range of 85 nm to 105 nm. This can be explained as zinc oxide ionic radii being much smaller than LSCF ionic radii, which results in the overall particle size being reduced. (Zinc ionic radius = 0.74 Å, LSCF = 1.4 Å).
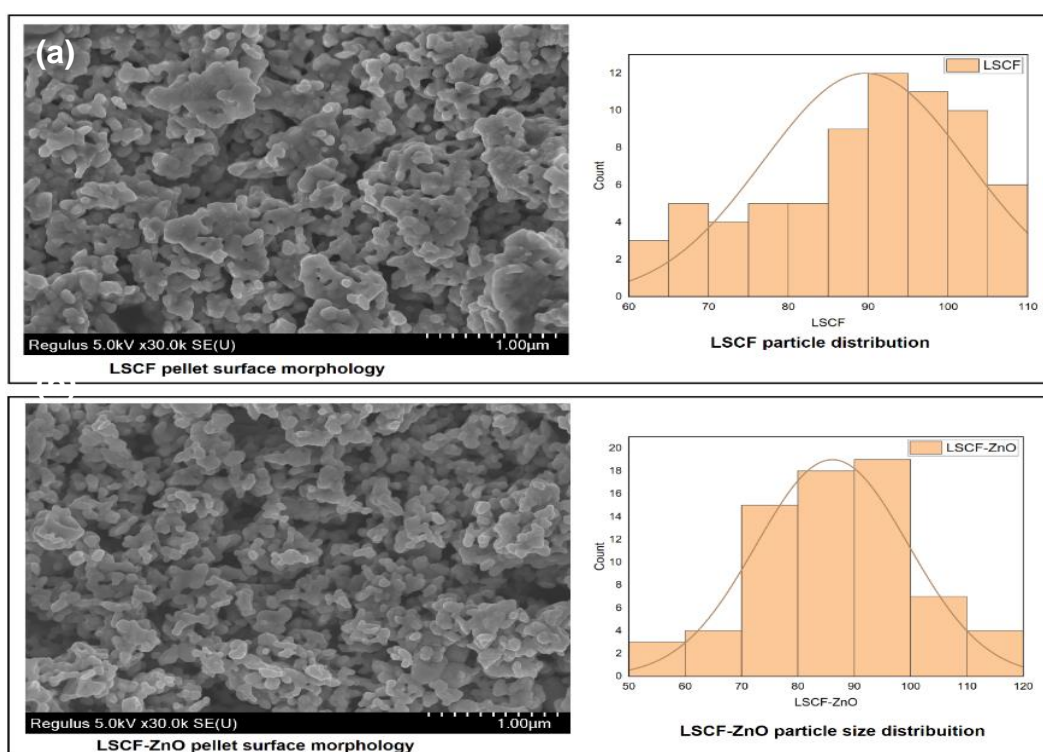

Figure 2 SEM images for the surface microstructure of (a) surface of bare LSCF cathode (b) surface of LSCF with 5 wt% of ZnO cathode

The TGA experiment was carried out using airflow to see how well they could fill/empty the oxygen content, as shown in Figure 3. The investigation was conducted at a range of 30 to 800 °C to imitate the oxygen filling/emptying capabilities when the device was used at an intermediate temperature range. The weight loss occurs between 30 and 100 °C, which is explained by the evacuation of absorbed water from the surrounding environment. The second section was seen for the entire sample after 200 °C, when there is a little weight rise, implying that Co^{3+}/Fe^{3+} is thermally oxidized to Co^{4+}/Fe^{4+}. This effect has also been described as the Co^{3+}/Fe^{3+} ions are generally difficult to convert to air, resulting in a minor weight gain and mass change. Table 1 summarizes the overall results of LSCF and LSCF-ZnO. The oxygen nonstoichiometric value of LSCF-ZnO was found to be greater than LSCF, implying that more oxygen reduction process occurs on the cathode.

**Table 1** Oxygen stoichiometric for LSCF and LSCF-ZnO

Sample	$M_{speciment}$ (g/mol)	M_{oxygen} (g/mol)	$\Delta m/m_s$	$\Delta\delta$
LSCF	222.860	16	0.750	0.100
LSCF-ZnO	300.070	16	0.810	0.150
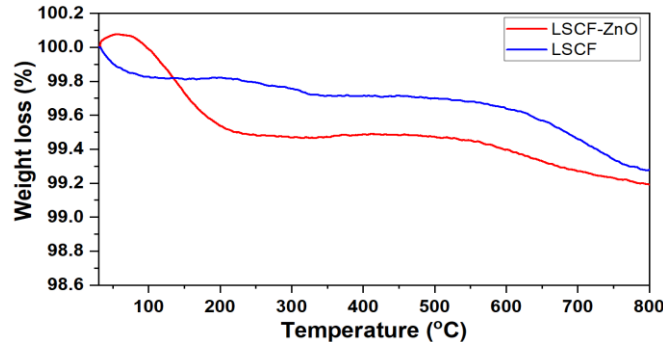
Figure 3 Weight loss graph of pure LSCF vs LSCF with 5 wt% ZnO powder

3.2. Electrochemical properties of the symmetrical composite cathode pellets

The electrochemical response of the LSCF-ZnO-modified electrode was measured via electrochemical impedance spectroscopy. Figure 4 (a) revealed the area-specific resistance (ASR) of LSCF symmetric cells with varied ZnO loading content at 800 °C. It was clear that the addition of zinc oxide up to 7 wt% towards the LSCF cathode was able to reduce the ASR at operating temperatures between 800 °C, indicating the oxygen reduction rate was improved by zinc oxide particles. The lowest ASR achieved from this analysis is LSCF with 5 wt% of zinc oxide (ASR = 0.045 cm^2) compared to pure LSCF (ASR = 0.088 cm^2) while operating at 800 °C. At 800 °C, the addition of 5% zinc oxide to LSCF reduces the ASR from 0.088 Ω cm^2 to 0.045 Ω cm^2. When the addition of zinc oxide increased to 7 wt% and 9 wt%, the ASR showed a slight increase at 7 wt% (ASR = 0.051 Ω cm^2), while a major increase was recorded at 9 wt% (ASR = 0.14 Ω cm^2), which is even higher than pure LSCF.

Figure 4 (b) summarizes the total ASR performance and shows that adding 5 wt% of zinc oxide resulted in the lowest overall ASR up to 600 °C operating temperature. It was found that up to 650 °C operating temperature, adding 7 wt% zinc oxide produced ASR readings that were comparable to LSCF with 5 wt% ZnO. When LSCF with 7 wt% ZnO was operated at 600 °C, there was a discernible difference in the ASR. Based on prior comparisons of ASR at 800 °C, the ASR gap value is regarded as large for the operating temperature of 600 °C (1.460 Ω cm^2 for LSCF+ 5 wt% ZnO, and 1.710 Ω cm^2 for LSCF+ 7 wt% ZnO), even though there is a slight variation between 800 °C and 650 °C.
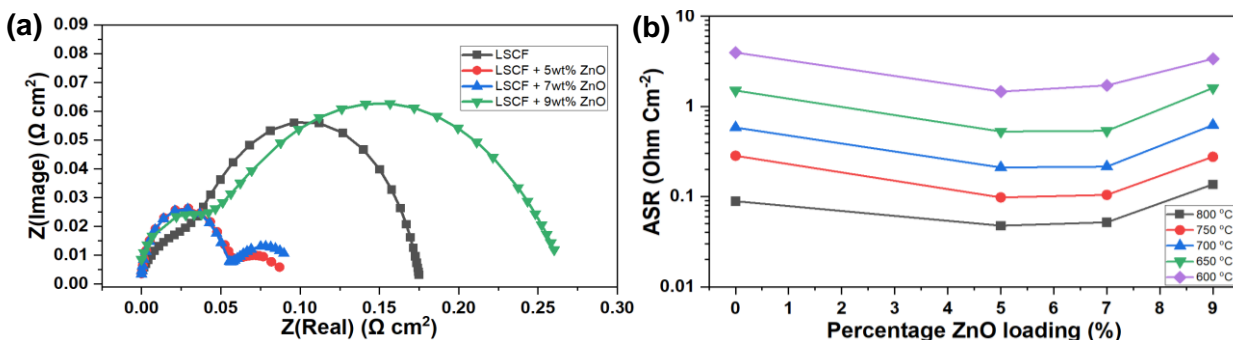
Figure 4 The impedance spectroscopy of pure LSCF and LSCF with different wt% ZnO loading at operating temperature 800 °C (a) Effect of zinc oxide addition on LSCF cathode towards the ASR of the symmetric cell (b)

In this case, it is important to observe the overall performance of the area-specific resistance (ASR) at intermediate temperatures in order to determine the optimal value for zinc oxide addition. As exponential growth of ASR was observed after the 600 °C operating temperature, the lowest ASR for intermediate temperatures was found to be achieved with a 5 wt% zinc oxide loading (ASR LSCF with 5 wt% ZnO = 1.460 Ω cm^2). Based on the ASR and specific surface area analysis, it can be concluded that adding 5 wt% zinc oxide to LSCF provides the best performance.

Brunauer-Emmett-Teller (BET) was conducted to measure the specific surface area of the LSCF with the addition of 3%, 5%, 7%, and 9% of zinc oxide, respectively. A higher active surface area is desired to simulate the higher capability of oxygen reduction reaction (ORR) in the cathode. It is found that 3 wt% of zinc oxide slightly increased the S_{BET} of LSCF from 7.510 m^3/g to 7.920 m^3/g, while a significant increment was observed after zinc oxide content was increased up to 5 wt% (S_{BET} = 10.520 m^3/g). A slight decrease of S_{BET} up to 10.340 m^3/g was observed at 7 wt% addition of zinc oxide towards the LSCF cathode, and the S_{BET} was dropped to 9.950 m^3/g after 9 wt% of zinc oxide addition towards LSCF. The data trends show remarkably similar to EIS analysis where the 5% of ZnO toward LSCF gave the best result among other candidates, and the performance dropped after the ZnO loading exceeded 5%. The specific surface area for LSCF-ZnO also was higher than several LSCF-based composite cathodes from other literature (LSCF-GDC=8.010 m^3/g (Xi *et al.*, 2016), LSCF-CuO=8.150 (Fatah and Hamid, 2018), LSCF-YSZ=5.52 (Cai *et al.*, 2018).

The electrochemical impedance spectra with bode phase analysis were conducted with pure LSCF and LSCF with 5 wt% of ZnO at 800 °C to prove that improvement in ORR of LSCF-ZnO cathode. Figure 5 (a) shows the Nyquist plot for pure LSCF symmetric cell and LSCF with 5 wt% of ZnO symmetric cell with subtraction of resistance related to silver wire and electrolyte for better comparison. At 800 °C, the ASR for the pure LSCF was reduced from 0.089 cm^2 to 0.047 cm^2 after the addition of 5 wt% zinc oxide. The Bode phase plot revealed the position peak of pure LSCF and LSCF-ZnO at 800 °C was plotted in Figure 5 (b). The curve fit represents the existence of two peaks (P1 and P2), which correspond to the Nyquist plot with the corresponding frequency. P1 (low frequency) represents the ORR process that occurred at the triple boundary phase of the cathode, while P2 (high frequency) embodies the charge transfer that occurred on the grain boundary (Ali *et al.*, 2017). It was observed that the ASR of P2 slightly increased from 0.019 cm^2 to 0.022 cm^2 after the addition of 5 wt% zinc oxide due to the LSCF pore's structure being blocked by zinc oxide, which subsequently hindered the charge transfer process, which is also associated with bulk transport of oxide-ions at the cathode. In conjunction with this study, the P1 shows a massive ASR reduction from 0.070 cm^2 to 0.025 cm^2 after the addition of 5 wt% zinc oxide, which verified that the addition of zinc oxide could improve the oxygen reduction reaction process of the LSCF electrode. It was expected for the P1 for LSCF-ZnO to outperform bare LSCF as the addition of ZnO was capable of improving the specific surface area of the cathode which was previously shown in BET analysis. Although it slightly increases the high-frequency ASR (P2), zinc oxide can improve the ORR process, which subsequently reduces the ASR greatly from 0.088 cm^2 to 0.045 cm^2.
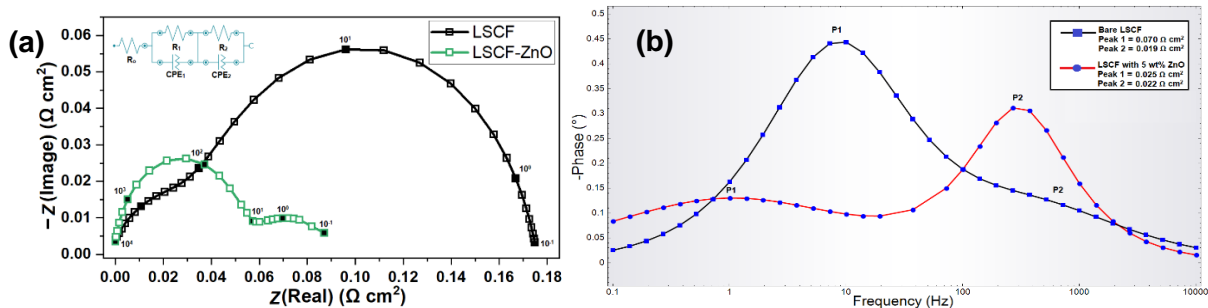
Figure 5 (a) Electrochemical impedance spectra measured at 800 °C for a pure LSCF symmetric cell and LSCF with 5 wt% ZnO symmetric cell and their respective bode phase results are shown in (b)

3.3. Electrochemical properties of the symmetrical composite cathode pellets

Figure 6 (a) displays the performance of single-cell configurations with pure LSCF and LSCF with 5 wt% ZnO at operating temperatures of 650 °C and 600 °C. Previously, the ASR analysis graph revealed significant increases in ASR value between 650 °C and 600 °C. Therefore, the performance analysis was conducted as low as 650 °C to measure the power density at the lowest operating temperature for the intermediate temperature range. The power density of the LSCF electrode was increased from 0.22 Wcm^{-2} to 0.27 Wcm^{-2} after the addition of 5 wt% of zinc oxide. As an example, for comparison performance by temperature, single cells of pure LSCF and LSCF with 5 wt% of zinc oxide were also conducted at a 600 °C operating temperature. It was measured that a major drop in power density occurred for pure LSCF compared to LSCF-ZnO, where the power density of pure LSCF dropped from 0.22 Wcm^{-2} to 0.09 Wcm^{-2}, which brought a 59% reduction in performance, while LSCF-ZnO performance reduction was only 45%. This agreed with the electrochemical analysis presented before, where the ASR of pure LSCF drastically increased at 600 °C operating temperature, while LSCF-ZnO showed a moderate decrease in ASR at similar temperatures. This validates that LSCF-ZnO is capable of being operated as low as 600 °C, where the addition of zinc oxide still enhances the ORR process on the LSCF structure.

The enhancement made by the LSCF-ZnO cathode in single-cell performance indicates that zinc addition indeed enhances the ORR kinetics of the LSCF cathode. Figure 6 (b) finalizes the electrochemical performance analysis where the activation energy of pure LSCF was compared with LSCF with (5 wt%, 7 wt%, and 9 wt%) of zinc oxide addition. It was concluded that LSCF with 5 wt% of ZnO is the most sensible value for LSCF-ZnO cathode fabrication. Although the result of 7 wt% ZnO produced a nearly identical response to the 5 wt% ZnO, the ASR value of LSCF-ZnO (7 wt%) at 600 °C shows a significant increase compared to LSCF-ZnO (5 wt%), putting LSCF-ZnO (5 wt%) as the best choice in this study.
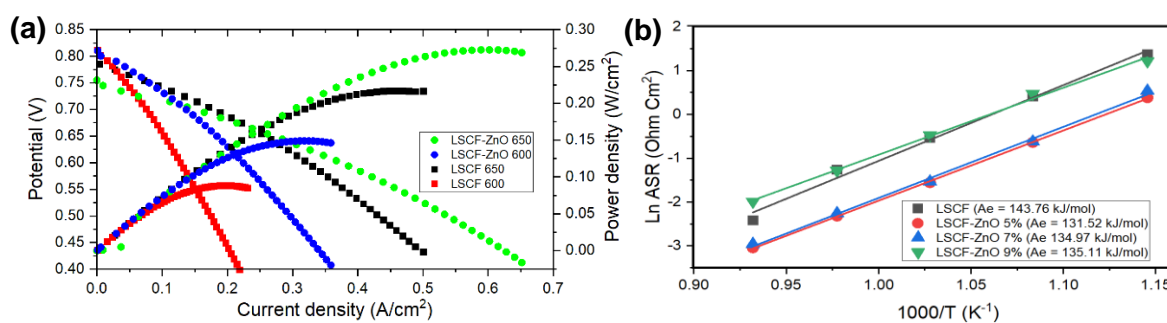
Figure 6 Cell voltage and power density for a single cell LSCF cathode and LSCF cathode with 5 wt% addition of ZnO at 650 °C and 600 °C operating temperature (a) and activation energy of bare and varies wt% of ZnO in LSCF (b)

4. Conclusions

The addition of zinc oxide to the LSCF cathode was shown to improve the catalytic activity for oxygen reduction reaction (ORR). LSCF-ZnO was successfully synthesized using the modified sol-gel method, ensuring that no solid-state reaction occurred between the two phases. It was then observed that the addition of 5 wt.% zinc oxide toward LSCF capable of reducing the ASR value from 0.088 Ω cm^2 to 0.045 Ω cm^2 and among 5 wt.%, 7 wt.% and 9 wt.% of zinc oxide, 5 wt.% of zinc oxide toward LSCF give the lowest ASR value throughout the intermediate temperature operation (800 °C -600 °C). Further analysis revealed that S$_{Bet}$ of LSCF-ZnO is indeed higher than pure LSCF overall. The Bode phase confirms the ASR value of LSCF-ZnO drastically reduced for low-frequency resistance, indicating major improvement of the ORR process, which subsequently improves the triple boundary phase of the cathode. Single-cell performance of LSCF with 5 wt.% of zinc oxide at 650 °C revealed improvement from 0.220 W cm^{-2} to 0.270 W cm^{-2}. This agrees well with specific surface area analysis and electrochemical analysis of LSCF-ZnO symmetric cell where the specific surface area increased drastically from 7.510 m^3/g to 10.520 m^3/g after 5 wt.% of ZnO was added into LSCF cathode. The Bode phase from electrochemical analysis further elaborated that major reduction or low-frequency ASR (P1) from 0.070 Ω cm^2 to 0.025 Ω cm^2 proves that zinc oxide is capable of enhancing the ORR process.

Acknowledgments

References

Abbas, G., Ahmad, M.A., Raza, R., Aziz, M.H, Khan, M.A., Hussain, F., Sherazi, T.A. 2019. Fabrication of High Performance Low Temperature Solid Oxide Fuel Cell Based on La$_{0.10}$Sr$_{0.90}$Co$_{0.20}$Zn$_{0.80}$O$_{5-\delta}$ Cathode. *Materials Letters,* Volume 238, pp. 179–182

Abd-Aziz, A.J., Baharuddin, N.A., Somalu, M.R., Muchtar, A. 2020. Review of Composite Cathodes For Intermediate-Temperature Solid Oxide Fuel Cell Applications. *Ceramics International,* Volume 46, pp. 23314–23325

Adiwibowo, M.T., Ibadurrohman, M., Slamet, S. 2018. Synthesis of Zno Nanoparticles and their Nanofluid Stability in the Presence of a Palm Oil-Based Primary Alkyl Sulphate

Surfactant for Detergent Application. *International Journal of Technology,* Volume 9, pp. 307–316

Ali, S.M., Anwar, M., Somalu, M.R., Muchtar, A. 2017. Enhancement of The Interfacial Polarization Resistance of $La_{0.6}Sr_{0.4}Co_{0.2}Fe_{0.8}O_{3-\Delta}$ Cathode by Microwave-Assisted Combustion Method. *Ceramics International,* Volume 43(5), pp. 4647–4654

Cai, Y., Wang, B., Wang, Y., Xia, C., Qiao, J., Van Aken, P.A., Zhu, B., Lund, P., 2018. Validating The Technological Feasibility of Yttria-Stabilized Zirconia-Based Semiconducting-Ionic Composite in Intermediate-Temperature Solid Oxide Fuel Cells. *Journal of Power Sources,* Volume 384, pp. 318–327

Dos Santos-Gómez, L., Porras-Vázquez, J.M., Losilla, E.R., Martín, F., Ramos-Barrado, J.R., Marrero-López, D., 2018. LSCF-CGO Nanocomposite Cathodes Deposited in A Single Step by Spray-Pyrolysis. *Journal of the European Ceramic Society,* Volume 38, pp. 1647–1653

Dumaisnil, K., Fasquelle, D., Mascot, M., Rolle, A., Roussel, P., Minaud, S., Duponchel, B., Vannier, R.N., Carru, J.C., 2014. Synthesis and Characterization of $La_{0.6}Sr_{0.4}Co_{0.8}Fe_{0.2}O_3$ Films For Solid Oxide Fuel Cell Cathodes. *Thin Solid Films,* Volume 553, pp. 89–92

Fatah, A.F., Hamid, N.A., 2018. Physical and Chemical Properties Of LSCF-Cuo as Potential Cathode for Intermediate Temperature Solid Oxide Fuel Cell (IT-SOFC). *Malaysian Journal of Fundamental and Applied Sciences,* Volume 14, pp. 391–396

Gao, C., Liu, Y., Xi, K., Jiao, S., Tomov, R.I., Kumar, R.V., 2017. Improve the Catalytic Property of $La_{0.6}Sr_{0.4}Co_{0.2}Fe_{0.8}O_3/Ce_{0.9}Gd_{0.1}O_2$ (LSCF/CGO) Cathodes with Cuo Nanoparticles Infiltration. *Electrochimica Acta,* Volume 246, pp. 148–155

Guo, S., Wu, H., Puleo, F., Liotta, L., 2015. B-Site Metal (Pd, Pt, Ag, Cu, Zn, Ni) Promoted $La_{1-x}Sr_xCo_{1-y}Fe_yO_{3-\delta}$ Perovskite Oxides as Cathodes for IT-SOFCs. *Catalysts,* Volume 5, pp. 366–391

Hajmohammadi, M.R., Aghajannezhad, P., Abolhassani, S.S., Parsaee, M., 2017. An Integrated System of Zinc Oxide Solar Panels, Fuel Cells, and Hydrogen Storage for Heating And Cooling Applications. *International Journal of Hydrogen Energy,* Volume 42, pp. 19683–19694

Hussain, F., Abbas, G., Ahmad, M.A., Raza, R., Rehman, Z.U., Mumtaz, S., Akbar, M., Riaz, R.A., Dilshad, S., 2019. Comparative Electrochemical Investigation of Zinc Based Nano-Composite Anode Materials for Solid Oxide Fuel Cell. *Ceramics International,* Volume 45, pp. 1077–1083

Jiang, S.P., 2019. Development of Lanthanum Strontium Cobalt Ferrite Perovskite Electrodes of Solid Oxide Fuel Cells – A Review. *International Journal of Hydrogen Energy,* Volume 44, pp. 7448–7493

Kusdianto, K., Widiyastuti, W., Shimada, M., Nurtono, T., Machmudah, S., Winardi, S., 2019. Photocatalytic Activity of ZnO-Ag Nanocomposites Prepared by a One-step Process using Flame Pyrolysis. *International Journal of Technology,* Volume 10, pp. 571–581

Nadeem, M., Hu, B., Xia, C., 2018. Effect of NiO Addition on Oxygen Reduction Reaction at Lanthanum Strontium Cobalt Ferrite Cathode for Solid Oxide Fuel Cell. *International Journal of Hydrogen Energy,* Volume 43, pp. 8079–8087

Omari, E., Omari, M., Barkat, D., 2018. Oxygen evolution reaction over copper and zinc co-doped LaFeO3 perovskite oxides. *Polyhedron,* Volume 156, pp. 116–122

Rafique, A., Raza, R., Ali, A., Ahmad, M.A., Syväjärvi, M., 2019. An Efficient Carbon Resistant Composite $Ni_{0.6}Zn_{0.4}O_{2-\Delta}$-GDC Anode for Biogas Fuelled Solid Oxide Fuel Cell. *Journal of Power Sources,* Volume 438, pp. 227042–227052

Samreen, A., Galvez-Sanchez, M., Steinberger-Wilckens, R., Arifin, N.A., Saher, S., Ali, S., Qamar, A. 2020. Electrochemical Performance of Novel NGCO-LSCF Composite Cathode

for Intermediate Temperature Solid Oxide Fuel Cells. *International Journal of Hydrogen Energy,* Volume 45, pp. 21714–21721

Shah, M.A.K.Y., Mushtaq, N., Rauf, S., Xia, C., Zhu, B., 2019. The Semiconductor SrFe$_{0.2}$Ti$_{0.8}$O$_{3-\Delta}$-Zno Heterostructure Electrolyte Fuel Cells. *International Journal of Hydrogen Energy,* Volume 44(57), pp. 30319–30327

Tahir, N.N.M., Baharuddin, N.A., Samat, A.A., Osman, N., Somalu, M.R., 2022. A Review on Cathode Materials for Conventional and Proton-Conducting Solid Oxide Fuel Cells. *Journal of Alloys and Compounds,* Volume 894, pp. 162458–162474

Wu, X.Y., Ghoniem, A.F., 2019. Mixed Ionic-Electronic Conducting (MIEC) Membranes for Thermochemical Reduction of CO$_2$: A Review. *Progress in Energy and Combustion Science,* Volume 74, pp. 1–30

Xi, X., Kondo, A., Kozawa, T., Naito, M., 2016. LSCF–GDC Composite Particles for Solid Oxide Fuel Cells Cathodes Prepared by Facile Mechanical Method. *Advanced Powder Technology,* Volume 27, pp. 646–651

Xu, Q., Guo, Z., Xia, L., He, Q., Li, Z., Bello, I.T., Zheng, K., Ni, M., 2022. A Comprehensive Review of Solid Oxide Fuel Cells Operating on Various Promising Alternative Fuels. *Energy Conversion and Management,* Volume 253, pp. 115175–115222

Xu, S., Liu, J., Zhou, Y., Yang, S., Zhang, R., Yang, X., Xu, D., 2020. Processing and Conduction Properties of Gd-Doped Ceria Electrolytes with ZnO Semiconductor. *Solid State Ionics,* Volume 358, pp. 115505–115511